

# An algorithm for learning sparsifying transforms of multidimensional signals

## Algoritmo de aprendizaje de diccionarios para transformación de imágenes multidimensionales en señales dispersas

Oscar Enrique Hurtado-Camacho<sup>1</sup>, Hoover Fabián Rueda-Chacon<sup>2</sup>, Henry Arguello-Fuentes<sup>1\*</sup>



<sup>1</sup> Escuela de Ingeniería de Sistemas e Informática, Universidad Industrial de Santander. Carrera 27, Calle 9. C. P. 680002. Bucaramanga, Colombia.

<sup>2</sup> Department of Electrical and Computer Engineering, University of Delaware. Room 140 Evans Hall. 19716. Newark, DE, USA.

### ARTICLE INFO

Received May 17, 2016  
Accepted April 19, 2017

### KEYWORDS

Sparse representation, dictionary learning, sparsifying transforms, multidimensional signal processing

Representación escasa, aprendizaje de diccionarios, transformadas para escasez, procesamiento de imágenes multidimensionales

**ABSTRACT:** Multidimensional signals contain information of an object in more than one dimension, and usually their processing relies on complex methods in comparison with their unidimensional counterparts. In signal processing, finding a sparse representation of a signal is of great importance for compression purposes. Analytical multidimensional bases such as the Fourier, Cosine, or Wavelet Transform have been conventionally used. Recently, the use of learned dictionaries that directly adapt to the given signal are becoming popular in tasks such as image classification, image denoising, spectral unmixing, and medical image reconstruction. This paper presents an algorithm to learn transformation bases for the sparse representation of multidimensional signals. The proposed algorithm alternates between a sparse coding step solved by hard or soft thresholding strategies, and an updating dictionary step solved by a conjugate gradient method. Furthermore, the algorithm is tested using both: two-dimensional and three-dimensional patches, which are compared in terms of the sparsity performance for different types of multidimensional signals such as hyperspectral images, computerized axial tomography images and, magnetic resonance images. The attained results are compared against traditional analytical transforms and the state-of-the-art dictionary learning method: K-SVD.

**RESUMEN:** Las señales multidimensionales contienen información de un objeto en más de una dimensión y, comúnmente, su procesamiento requiere métodos de mayor complejidad que las señales unidimensionales. En procesamiento de señales, la representación escasa de una señal es de gran importancia para fines de compresión. Convencionalmente, transformaciones analíticas como las transformadas de Fourier, Coseno o Wavelet, han sido utilizadas. Recientemente, se ha popularizado el uso de diccionarios entrenados, que se adaptan a una señal dada, en aplicaciones como clasificación de imágenes, eliminación de ruido, separación espectral, y reconstrucción de imágenes médicas. Este artículo presenta un algoritmo para entrenar bases de transformación para representación escasa de señales multidimensionales. El algoritmo propuesto alterna entre una codificación escasa que se resuelve por umbralización, y la actualización del diccionario que se resuelve mediante el método de gradiente conjugado. Además, el artículo incluye una comparación entre parches bidimensionales y tridimensionales en términos del nivel de escasez que ofrecen en diferentes tipos de señales multidimensionales como: imágenes hiperespectrales, imágenes de tomografía computarizada, e imágenes de resonancia magnética. Los resultados obtenidos son comparados contra transformaciones analíticas tradicionales y contra el método de entrenamiento de diccionarios más conocido en el estado del arte: K-SVD.

## 1. Introduction

### 1.1. Motivation

Multidimensional signals are an important class of signals which are widely used in diverse applications such as medical imaging [1, 2], spectral remote sensing for target detection, classification or unmixing of substances [3, 4] and spectral imaging [5]. In these applications, the signals exhibit a

\* Corresponding author: Henry Arguello Fuentes  
e-mail: henarfu@uis.edu.co  
ISSN 0120-6230  
e-ISSN 2422-2844



multidimensional structure, where each dimension has a physical meaning e.g., space, time, frequency, wavelength. As a consequence, these signals contain more information about a phenomenon, and their processing is expensive in terms of computational complexity compared to unidimensional signals. In this regard, a tool in signal processing to deal with this problem is the sparsity. A signal is sparse if its energy is concentrated in just a few number of its coefficients [6]. Natural signals and images are not commonly sparse, but they could have a sparse representation by using an appropriate basis or dictionary [7, 8]. The sparse representation of signals has long been exploited in signal and imaging processing for various tasks such as compression, denoising [9, 10], and compressive sensing [8, 11]. The most popular dictionaries to obtain sparse representations are the ones obtained through the use of the Discrete Cosine Transform (DCT), and the Wavelet transform [12]. This kind of dictionaries are called analytical dictionaries given that they model the signals through the use of mathematical functions, which allow fast and implicit implementations to obtain useful representations. However, these representations are as accurate as the underlying model allows it, because the model needs to cope with the complexity of the natural phenomena, and in reality these models are inclined to be simple [13]. The learning dictionaries approach exists since they fit a given model, in particular with more accuracy, thus extracting information directly from the data itself.

## 1.2. Related work

In the literature, there exists two main models for the sparse representation of signals named the synthesis and the analysis models [14]. The synthesis sparse coding problem is the most popular and it states that a signal  $\mathbf{y} \in \mathbb{R}^n$  can be represented in a dictionary  $\mathbf{D} \in \mathbb{R}^{n \times d}$  as a linear combination of a few elemental columns, called *atoms* [9, 13]. This means that the signal can be obtained as  $\mathbf{y} = \mathbf{D}\mathbf{x}$ , where  $\mathbf{x} \in \mathbb{R}^d$  is the sparse representation, with  $\|\mathbf{x}\|_0 \ll d$ , where  $\|\cdot\|_0$  is the  $l_0$  quasi-norm that counts the non-zero entries of a vector. In this model, the sparse representation  $\mathbf{x}$  can be obtained by solving the optimization problem in Eq. (1) [6, 15]

$$\min_{\mathbf{x}} \|\mathbf{y} - \mathbf{D}\mathbf{x}\|_2^2, \quad \text{s.t.} \|\mathbf{x}\|_0 \leq s, \quad (1)$$

where  $s$  is the desired sparsity level of the representation,  $\|\cdot\|_2$  is the  $l_2$  norm ( $\|\mathbf{a}\|_2 = \sqrt{\sum_i |a_i|^2}$ ), and  $s \ll d$ . Finding the solution to this problem is non-deterministic polynomial-time hard (NP-hard). Despite of this, there are algorithms that can find a solution in polynomial time, under certain conditions [6, 15]. On the other hand, the analysis model states that a signal  $\mathbf{y}$  can be represented in an analysis dictionary  $\mathbf{\Omega} \in \mathbb{R}^{m \times n}$  via inner products with its rows, referred as *analysis atoms*, with  $\|\mathbf{\Omega}\mathbf{y}\|_0 = m - l$ , where  $\mathbf{\Omega}\mathbf{y} \in \mathbb{R}^m$  is sparse, and  $l$  are its number of zeros, called the co-sparsity [16]. In contrast to the synthesis model, this model allows obtaining the representation just by multiplying the signal  $\mathbf{y}$  with the analysis dictionary  $\mathbf{\Omega}$ .

The sparse representation models can be adapted to train dictionaries from training signals. There exist various state-of-the-art works that explore dictionary learning using the synthesis approach [17, 18], and the analysis approach [19–21], but most of them have to solve a non-convex problem where finding a solution is NP-Hard. As an alternative to the two previously mentioned models, there exist the so called transform model [22]. This model states that a signal  $\mathbf{y}$  can be approximately represented in a sparse way in a transform basis  $\mathbf{W} \in \mathbb{R}^{m \times n}$ , as  $\mathbf{W}\mathbf{y} = \mathbf{x} + \mathbf{e}$ , where  $\mathbf{x} \in \mathbb{R}^m$  is sparse with  $\|\mathbf{x}\|_0 \ll m$ , and  $\mathbf{e}$  is the representation error in the transform domain. This model is a generalization of the analysis model with  $\mathbf{\Omega}\mathbf{y}$  exactly sparse and, unlike the analysis model, it allows the sparse representation  $\mathbf{x}$  not to be constrained to lie in the range space of the transform  $\mathbf{W}$  [22], which implies that the transform model is more general than the analysis model. Assuming that  $\mathbf{W}\mathbf{y} \approx \mathbf{x}$ , the problem of obtaining a sparse representation  $\mathbf{x}$ , given a sparsity level  $s$  for a signal  $\mathbf{y}$  with a known transform basis  $\mathbf{W}$  can be formulated as in Eq. (2)

$$\min_{\mathbf{x}} \|\mathbf{W}\mathbf{y} - \mathbf{x}\|_2^2, \quad \text{s.t.} \|\mathbf{x}\|_0 \leq s. \quad (2)$$

The corresponding solution to the problem in Eq. (2) is obtained by hard thresholding  $\mathbf{W}\mathbf{y}$ , i.e. by retaining its  $s$  largest coefficients. In comparison, the synthesis and analysis models, need to solve the sparse coding problem, dealing with NP-hard problems.

The transform model in Eq. (2) can be generalized in order to obtain a sparsifying transform  $\mathbf{W}$  from a matrix of training signals  $\mathbf{Y} \in \mathbb{R}^{n \times N}$  with sparse representation  $\mathbf{X}$ , such that each column represents a training signal, with  $N$  as the number of training signals. Constraining the model to obtain a square transform can be formulated by minimizing the error given by  $\|\mathbf{W}\mathbf{Y} - \mathbf{X}\|_F^2$ , where  $\mathbf{W} \in \mathbb{R}^{n \times n}$ ,  $\mathbf{X} \in \mathbb{R}^{n \times N}$  [22], and by expressing it as in Eq. (3)

$$\min_{\mathbf{W}, \mathbf{X}} \|\mathbf{W}\mathbf{Y} - \mathbf{X}\|_F^2 - \lambda \log \det \mathbf{W} + \mu \|\mathbf{W}\|_F^2, \quad \text{s.t.} \|\mathbf{X}_i\|_0 \leq s \quad \forall i, \quad (3)$$

where  $\mathbf{X}$  is column-sparse, and  $\|\cdot\|_F$  is the Frobenius norm ( $\|\mathbf{A}\|_F = \sqrt{\sum_i \sum_j |a_{ij}|^2}$ ). Note that, in Eq. (3) the  $\log \det \mathbf{W}$  term penalizes the transforms with small determinants, helping to obtain a full rank transform  $\mathbf{W}$ , thus avoiding trivial solutions, such as those composed by repeated rows. Similarly, the  $\|\mathbf{W}\|_F^2$  term helps to control the condition number of the transform  $\mathbf{W}$  [22].

In this paper, we propose an algorithm to learn sparsifying transforms from multidimensional signals based on the transform model given in Eq. (3). The proposed algorithm exhibits better performance than analytical transforms for sparse representations, and in contrast to synthesis or analysis dictionary learning strategies, the transform model allows approximating  $\mathbf{W}\mathbf{Y}$  by a column-sparse matrix  $\mathbf{X}$ , leading to a simpler, faster and cheaper implementation.

## 2. Proposed algorithm

In this section, an algorithm is proposed to solve the problem in Eq. (3). This algorithm alternates between two stages, a sparse coding stage in which the problem seeks to find sparse representations  $\mathbf{X}$  of the training signals  $\mathbf{Y}$ , fixing the transform basis  $\mathbf{W}$ ; followed by a dictionary update stage, where the transform  $\mathbf{W}$  is updated by fixing the just found sparse representation  $\mathbf{X}$ . The stages are detailed as follows:

### 2.1. Sparse coding step

In this step Eq. (3) is solved by fixing the dictionary  $\mathbf{W}$ . This can be written as Eq. (4)

$$f(\mathbf{X}) = \min_{\mathbf{X}} \|\mathbf{WY} - \mathbf{X}\|_F^2, \quad \text{s.t. } \|\mathbf{X}_i\|_0 \leq s \quad \forall i. \quad (4)$$

An easier problem than that in Eq. (4) can be obtained by relaxing the  $\ell_0$  quasi-norm constraint to the  $\ell_1$  norm, moving it to the objective function using Lagrange multipliers. The resulting optimization problem can be formulated as in Eq. (5)

$$f(\mathbf{X}) = \min_{\mathbf{X}} \|\mathbf{WY} - \mathbf{X}\|_F^2 + \eta \sum_{i=1}^N \|\mathbf{X}_i\|_1, \quad (5)$$

where  $\eta$  is a regularization parameter, and  $\|\cdot\|_1$  represents the  $\ell_1$  norm. The relaxed problem in Eq. (5) can then be solved through a soft thresholding as presented in Eq. (6)

$$\mathbf{X}_{ij} = \begin{cases} (\mathbf{WY})_{ij} - \frac{\eta}{2}, & (\mathbf{WY})_{ij} \geq \frac{\eta}{2} \\ (\mathbf{WY})_{ij} + \frac{\eta}{2}, & (\mathbf{WY})_{ij} < -\frac{\eta}{2} \\ 0, & \text{otherwise} \end{cases} \quad (6)$$

where the subscripts  $ij$  index the matrix entries. An alternative solution to the optimization problem in Eq. (4) can be obtained by hard thresholding, that is, by maintaining the  $s$  largest coefficients in each of the columns of  $\mathbf{WY}$  [22].

### 2.2. Dictionary update step

This step involves solving Eq. (3) by fixing the previously found sparse representation matrix  $\mathbf{X}$ . This solution can be modeled as the unconstrained non-convex optimization problem in Eq. (7)

$$f(\mathbf{W}) = \min_{\mathbf{W}} \|\mathbf{WY} - \mathbf{X}\|_F^2 - \lambda \log \det \mathbf{W} + \mu \|\mathbf{W}\|_F^2. \quad (7)$$

A solution to problem in Eq. (7) can be found using algorithms such as the steepest descent, the conjugate gradient, among other mathematical optimization algorithms [23]. This work uses a conjugate gradient algorithm with backtracking line search given its faster convergence compared with steepest descent. To ease the process of finding the gradient of Eq. (7), we rewrite Eq. (7) as in Eq. (8),

$$f(\mathbf{W}) = \min_{\mathbf{W}} \text{tr}((\mathbf{WY} - \mathbf{X})(\mathbf{WY} - \mathbf{X})^T) - \lambda \log \det \mathbf{W} + \mu \text{tr}(\mathbf{W}\mathbf{W}^T), \quad (8)$$

by using the fact that  $\|\mathbf{A}\|_F = \sqrt{\text{tr}(\mathbf{A}\mathbf{A}^T)}$ , where “ $\text{tr}(\cdot)$ ” represents the trace. Expanding Eq. (8) it is obtained Eq. (9) as,

$$\begin{aligned} f(\mathbf{W}) &= \min_{\mathbf{W}} \text{tr}((\mathbf{W}\mathbf{Y}\mathbf{Y}^T\mathbf{W}^T - \mathbf{W}\mathbf{Y}\mathbf{X}^T - \mathbf{X}\mathbf{Y}^T\mathbf{W}^T + \mathbf{X}\mathbf{X}^T) - \lambda \log \det \mathbf{W} \\ &\quad + \mu \text{tr}(\mathbf{W}\mathbf{W}^T)) \\ f(\mathbf{W}) &= \min_{\mathbf{W}} \text{tr}(\mathbf{W}(\mathbf{Y}\mathbf{Y}^T + \mu\mathbf{I})\mathbf{W}^T) - 2\text{tr}(\mathbf{W}\mathbf{Y}\mathbf{X}^T) + \text{tr}(\mathbf{X}\mathbf{X}^T) - \\ &\quad \lambda \log \det \mathbf{W} \end{aligned} \quad (9)$$

where the last line follows by the property of the trace being a linear mapping. Therefore, the gradient of the function  $f(\mathbf{W})$  in Eq. (9) is given by Eq. (10),

$$\nabla_{\mathbf{W}} f(\mathbf{W}) = 2\mathbf{W}\mathbf{Y}\mathbf{Y}^T + 2\mu\mathbf{W} - 2\mathbf{X}\mathbf{Y}^T - \lambda\mathbf{W}^{-T}, \quad (10)$$

by using the fact that  $\nabla_{\mathbf{A}} \text{tr}(\mathbf{A}\mathbf{A}^T) = 2\mathbf{A}$ , and  $\nabla_{\mathbf{A}} \log \det(\mathbf{A}) = \mathbf{A}^{-T}$ . For the conjugate gradient algorithm iterations, various stopping criteria can be selected, but based on empirically results, it is used a fixed number of iterations, due to the fast convergence of the algorithm. An initial  $\mathbf{W}$  transform with positive determinant must be chosen for the algorithm to work. The proposed algorithm is summarized in Algorithm 1.

---

#### Algorithm 1

---

- 1: Input: training signal matrix  $\mathbf{Y} \in \mathbb{R}^{n \times N}$ , parameters  $\lambda$ , and  $\mu$ , desired sparsity level  $s$ , number of iterations of overall algorithm  $k$
  - 2: Output: dictionary  $\mathbf{W} \in \mathbb{R}^{m \times n}$ , sparse representation  $\mathbf{X} \in \mathbb{R}^{n \times N}$
  - 3: Initialization: set  $\mathbf{W} = \mathbf{W}_i$
  - 4 for  $i = 1, \dots, k$  do
  - 5: Sparse coding: solve  $\min_{\mathbf{X}} \|\mathbf{WY} - \mathbf{X}\|_F^2, \quad \text{s.t. } \|\mathbf{X}_i\|_0 \leq s \quad \forall i$
  - 6: Dictionary update: solve  $\min_{\mathbf{W}} \|\mathbf{WY} - \mathbf{X}\|_F^2 - \lambda \log \det \mathbf{W} + \mu \|\mathbf{W}\|_F^2$
  - 8: end for
  - 9: Return:  $\mathbf{W}, \mathbf{X}$
- 

Solving the sparse coding and dictionary update problems could become computationally expensive for large signals. Therefore, we propose to use small-size non-overlapping patches to reduce the computational burden of the algorithm. The training signals  $\mathbf{Y}$  are then proposed to be vectorized patches of a certain three-dimensional image. Two setups were considered using non-overlapping patches taken from the three-dimensional images: two-dimensional (2D) and three-dimensional (3D) patches. The use of patches entail dictionaries that can adapt to high correlated training signals with similar sparsity, thus allowing more flexibility. An sketch of the patch extraction procedure is depicted in Figure 1. The two-dimensional patches consist of taking a predefined number of pixels along two dimensions with the remaining dimension fixed. The three-dimensional patches consist of taking a predefined number of pixels along the three dimensions of the images.

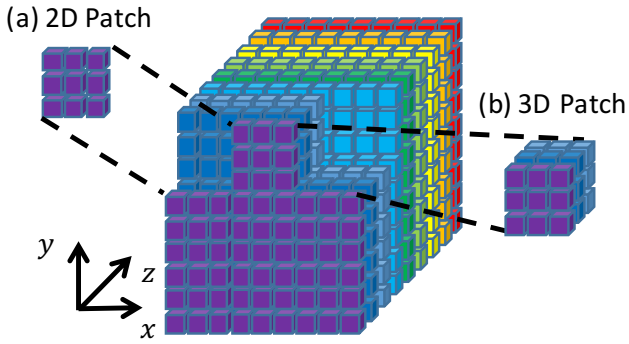


**Figure 1** Proposed setups for three-dimensional signals. a) 2D patch, b) 3D patch

Having an image as a three-dimensional array  $\mathbf{F} \in \mathbb{R}^{N \times M \times L}$ , it can be written in an indexed form as  $F_{i,j,k}$ , where  $i, j$  and  $k$  indexes are the two spatial and the spectral coordinate, respectively. The patches size in the spatial coordinate  $x$  is defined as  $p$ , and in the spatial coordinate  $y$  is defined as  $q$ . The vectorized 2D patches of the three-dimensional array are formulated as the  $l^{th}$  column of the training signal matrix  $\mathbf{Y}$  as given in Eq. (11)

$$(\mathbf{Y})_i = F_{i-\lfloor \frac{i}{p} \rfloor p + \lfloor \frac{i}{q} \rfloor q + (l \bmod u)q, \lfloor \frac{i}{p} \rfloor + (l \bmod u)q, \lfloor \frac{i}{uv} \rfloor}, \quad (11)$$

for  $i=0,1,\dots,pq-1, l=0,1,\dots,\frac{NML}{pq}-1$ , where  $v=\frac{N}{p}$ ,  $u=\frac{M}{q}$ , and "mod" is the modulo operation. For the 3D patches approach, a similar process is followed but additionally defining the patch size in the spatial coordinate  $z$  as  $r$ . The vectorized 3D patches of the three-dimensional array are then formulated as the  $l^{th}$  column of the training signal matrix  $\mathbf{Y}$  as in Eq. (12)

$$(\mathbf{Y})_i = F_{i-\lfloor \frac{i}{p} \rfloor p + \lfloor \frac{i}{qr} \rfloor qr, \lfloor \frac{i}{q} \rfloor - \lfloor \frac{i}{pq} \rfloor q + \lfloor \frac{i}{r} \rfloor r, \lfloor \frac{i}{pqr} \rfloor + (l \bmod t)r}, \quad (12)$$

for  $i=0,1,\dots,pqr-1, l=0,1,\dots,\frac{NML}{pqr}-1$ , where  $t=\frac{L}{r}$ .

### 3. Experiments

Several experiments with real multidimensional images were conducted to show the benefits of the proposed

algorithm. Experiments were performed using three test multidimensional signals shown in Figure 2: an hyperspectral image (HSI) composed of a section of a Lego scene with spatial resolution of  $128 \times 128$ , with 24 spectral bands [24]; a magnetic resonance image (MRI) composed of a resized scene of a head scan, property of the U.S. National Library of Medicine [25], with dimensions  $128 \times 128 \times 32$ ; and a computerized axial tomography scan (CAT) image of a human thorax acquired with a computed tomography scanner Toshiba Aquilion 64 with dimensions  $128 \times 128 \times 60$ .

The hyperspectral images are three-dimensional images consisting of large amounts of two dimensional spatial information of a scene across a multitude of spectral bands (wavelengths). In contrast, the magnetic resonance images are three-dimensional images with three spatial coordinates captured with a magnetic field and pulses of radio waves. Similarly, the computerized axial tomography images are three-dimensional images with three spatial coordinates captured using X-rays, to obtain projections at different angles with respect to an object of interest.

The size of the patches used for the 2D case was set to be  $8 \times 8$  pixels, and for the 3D patches was set to be  $8 \times 8 \times 4$  pixels. As used in common image processing applications [26], the mean of the patches (DC values) are removed prior to processing; that is, only mean-subtracted patches are processed, but the means are added back later only for display purposes. The proposed algorithm was run for a fix number of 20 iterations. The sparsity level of the signals was varied between 15% and 50%. For the sparse coding step, although soft thresholding is convex, the hard thresholding scheme was used due to the overhead to adjust the parameter  $\eta$  in Eq. (6). For the transform update step, the conjugate gradient algorithm was used and run for a fixed number of 10 iterations. The initial transform  $\mathbf{W}_1$  was chosen to be the 2D DCT matrix. An estimate of the training matrix is calculated as  $\hat{\mathbf{Y}} = \mathbf{W}^{-1}\mathbf{X}$ , and used to reconstruct the training multidimensional image. This output image is compared against the input multidimensional image in order to measure the quality of the results reached by the algorithm. The best parameters  $\lambda$  and  $\mu$  in Eq. (10) were found for each experiment by try-and-error running the algorithm multiple times.

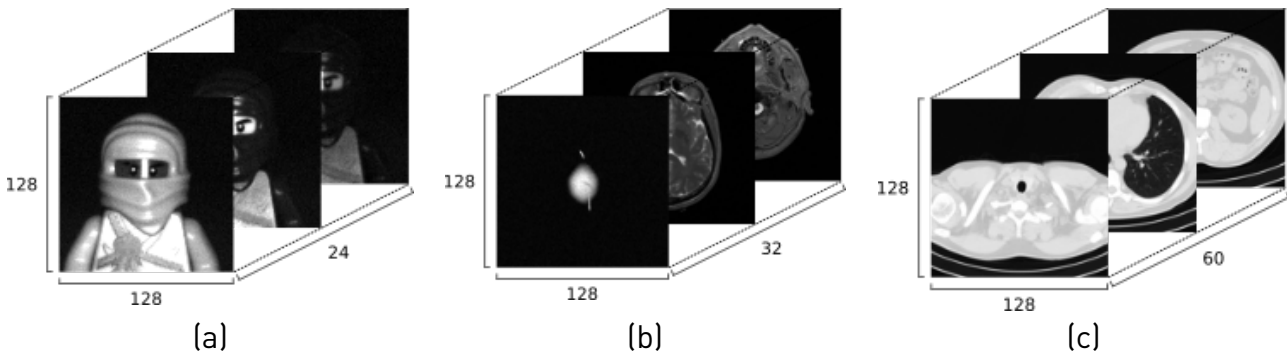


**Figure 2** Multidimensional training images. (a) HSI image with size  $128 \times 128 \times 24$ , (b) MRI image with size  $128 \times 128 \times 32$ , (c) CAT image with size  $128 \times 128 \times 60$

In particular, three sets of experiments were performed to test the proposed algorithm using the three multidimensional images shown in Figure 2. In the first experiment, we perform a sensitive analysis of the regularization parameters  $\lambda$  and  $\mu$ , seeking for the best values, since their correct selection highly impacts the final result. In the second experiment, we compare the performance of the proposed algorithm using either 2D and 3D patches with the best regularization parameters found in Experiment #1, against analytical transforms such as DCT and the identity, and the state of the art dictionary learning algorithm K-SVD [17]. In order to quantify the reconstruction quality of the multidimensional test images from the learned dictionary  $\mathbf{W}$ , the peak signal-to-noise ratio (PSNR) metric was calculated. The third experiment analyzes the concentration of the non-zero values of the signals after being represented on the attained dictionaries.

The higher the concentration of the non-zero values, the better the representation dictionary.

### 3.1. Experiment #1: Regularization parameters search

Figure 3 shows the performance of the algorithm for different sparsity settings between 15% and 50%, versus the value of the parameters  $\lambda$  and  $\mu$ , in terms of the PSNR of the reconstructed images attained from the estimation of the training matrix  $\hat{\mathbf{Y}}$ . The regularization parameters were varied in the interval  $[10^{-5}, 10^1]$ , and where set to be equal ( $\lambda = \mu$ ). The latter setting empirically proved to maintain a good leverage between the terms in the objective function. The parameters which yield the highest PSNR for each image are shown in Table 1, and these were chosen to be used for the rest of the experiments.

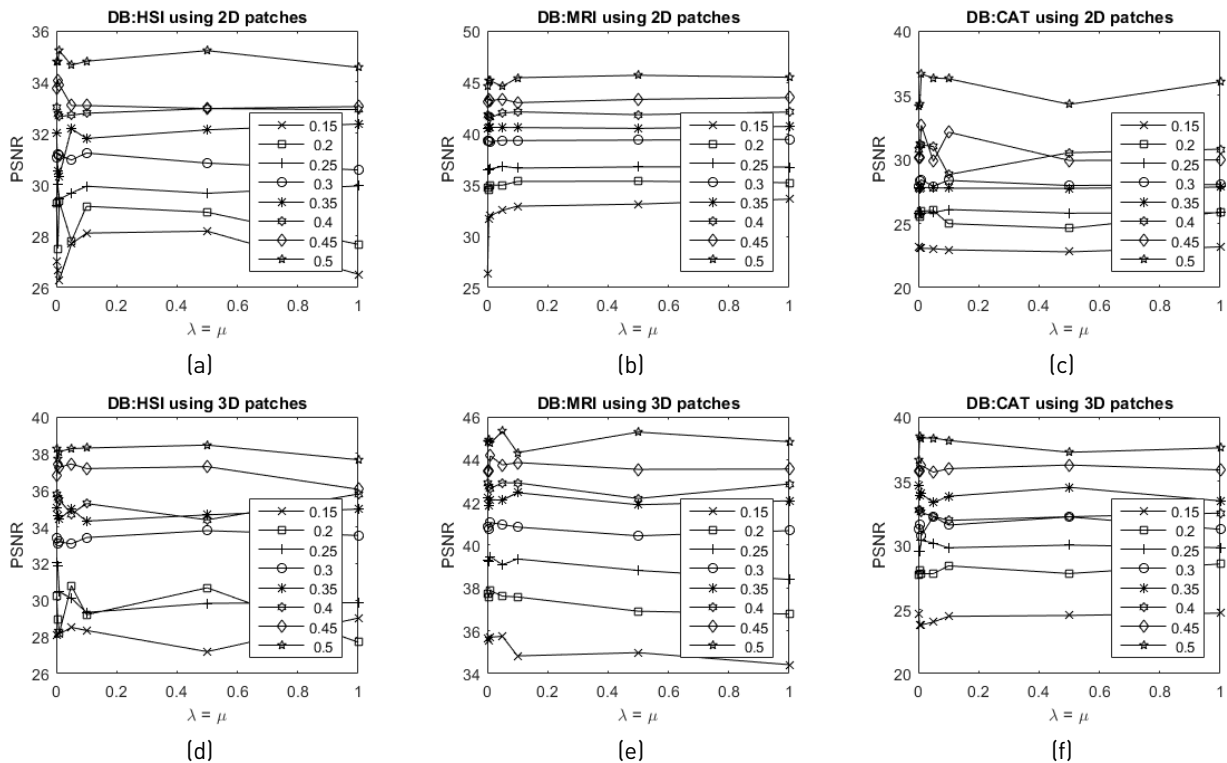


**Figure 3** Sensitive analysis of the regularization parameters  $\lambda$  and  $\mu$  for the different multidimensional test images in terms of PSNR, using 2D patches and 3D patches, respectively for (a-d) HSI image, (b-e) MRI image, and (c-f) CAT image

**Table 1** Best regularization parameters  $\lambda$  and  $\mu$  for the 3 test databases using 2D and 3D patches

Sparsity	2D Patches								3D Patches							
	.15	.20	.25	.30	.35	.40	.45	.50	.15	.20	.25	.30	.35	.40	.45	.50
HSI	5e-1	1e-2	5e-3	1e-1	1e0	1e-3	5e-3	1e-2	1e0	5e-2	1e-3	5e-1	1e-3	1e0	5e-2	5e-1
MRI	1e0	5e-1	5e-2	1e0	1e0	1e-1	1e0	5e-1	5e-2	1e-2	1e-2	1e-2	1e-1	5e-2	1e-2	5e-2
CAT	1e0	5e-2	1e-1	1e-2	1e0	5e-3	1e-2	1e-2	1e0	1e0	1e-2	5e-2	1e-3	1e-3	5e-1	5e-3

### 3.2. Experiment #2: Comparison with state-of-the-art methods

In order to test the accuracy of the proposed algorithm to create sparsifying dictionaries, we compare it against analytical dictionaries obtained through the DCT and the identity matrix. Moreover, we compare the proposed method against the widely-used state of the art dictionary learning algorithm K-SVD, which has shown to be reliable. Figure 4 summarizes several simulations that were performed varying the sparsity level of the signals to be represented by the dictionary. Note that the best regularization parameters were used for the proposed algorithm using either 2D or 3D patches, as given in Table 1.

In Figure 4, it can be observed that the analytical transforms generated from the identity matrix and the DCT perform worse than the dictionary learning algorithms, being the DCT dictionary the closest one. Comparing the dictionary learning methods, it can be seen that the K-SVD algorithm performs relatively well, since its attained PSNR results

are sandwiched between the behavior of the proposed algorithm using 2D and 3D patches. Remark that the use of 3D patches entails the best PSNR performance overall, confirming the assumptions that 3D patches represent better the correlations within high dimensional signals. In addition, Figure 4(a), 4(b) and 4(c) show that the compared algorithms seem to behave similarly no matter the number of slices of the multidimensional images being tested.

To evaluate the spatial quality of the reconstructed images based on the estimation of the training matrix, a comparison along the 2D spatial domain against the original test multidimensional images was made. Figures 5, 6 and 7 show zoomed versions of a single slice for each multidimensional test image, respectively, comparing the five methods listed in Figure 4, using different target sparsity levels. It can be confirmed from these figures that the proposed method using the 3D patches scheme performs best overall, for the three multidimensional images tested. Note however, that close results are attained by using the 2D patches scheme and the K-SVD algorithm.

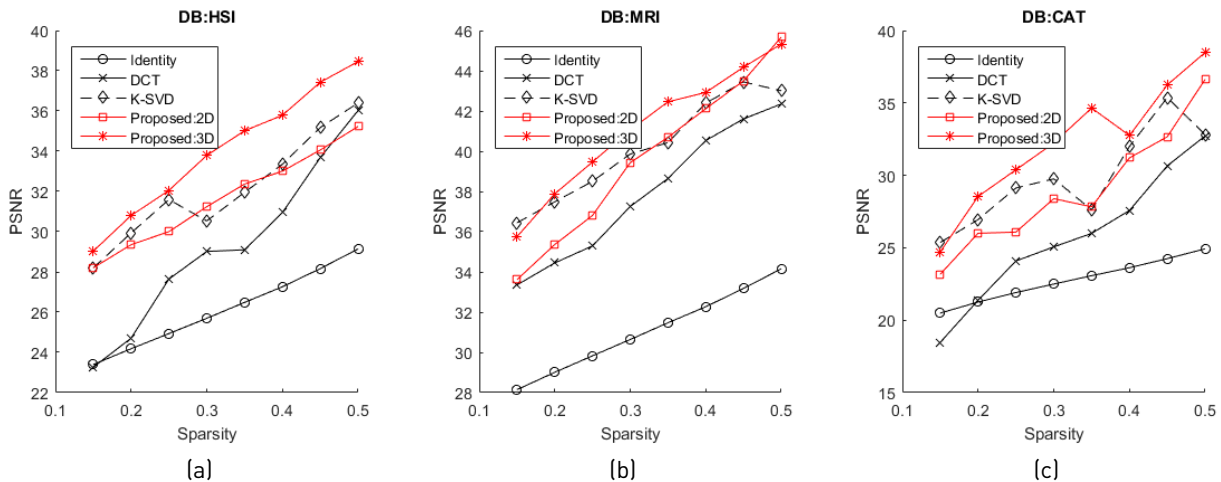


**Figure 4 Comparison between the proposed method, the DCT and identity analytical transforms, and the state of the art dictionary learning K-SVD algorithm for different sparsity levels, in terms of PSNR for the three multidimensional test databases**

In Figure 8, a comparison of the footprints of 6 different slices along the third dimension of the three test databases is shown, in order to analyze the performance of the best analytical (DCT), the K-SVD and the best proposed method

(using 3D patches). It can be observed from the figure that each algorithm performs consistently along the third dimension, with the K-SVD and the proposed method attaining the best quality.

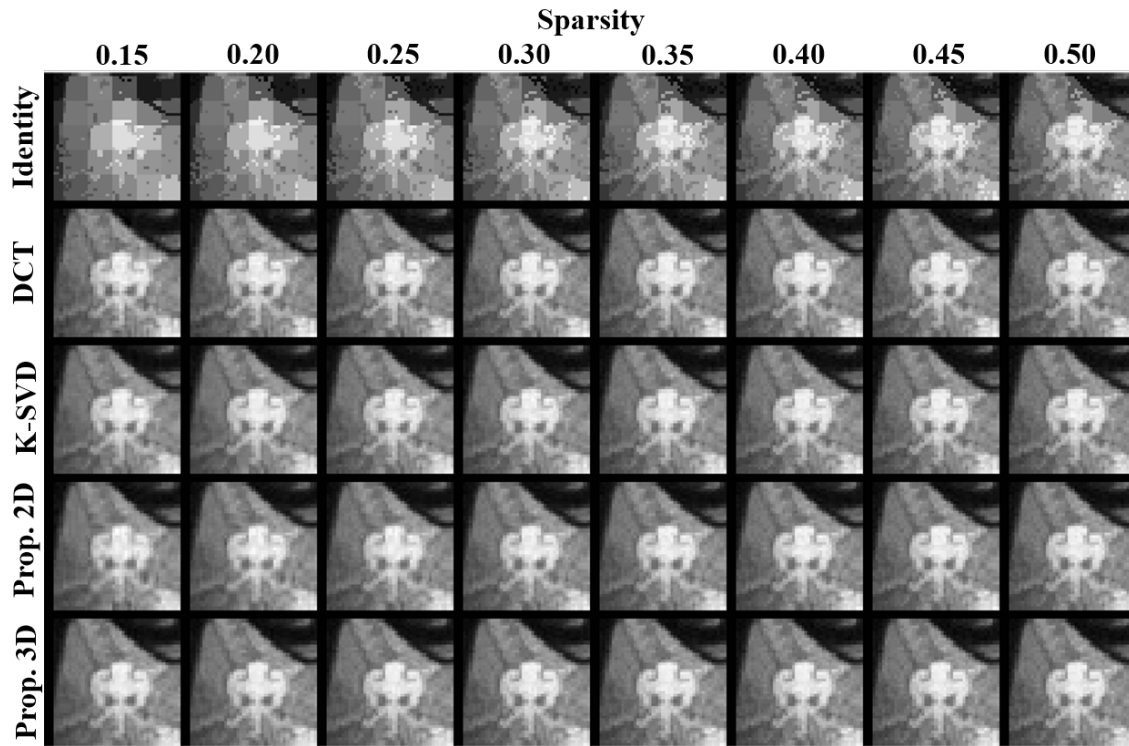


Figure 5 Comparison of the 15<sup>th</sup> slice of the HSI database for different sparsity levels

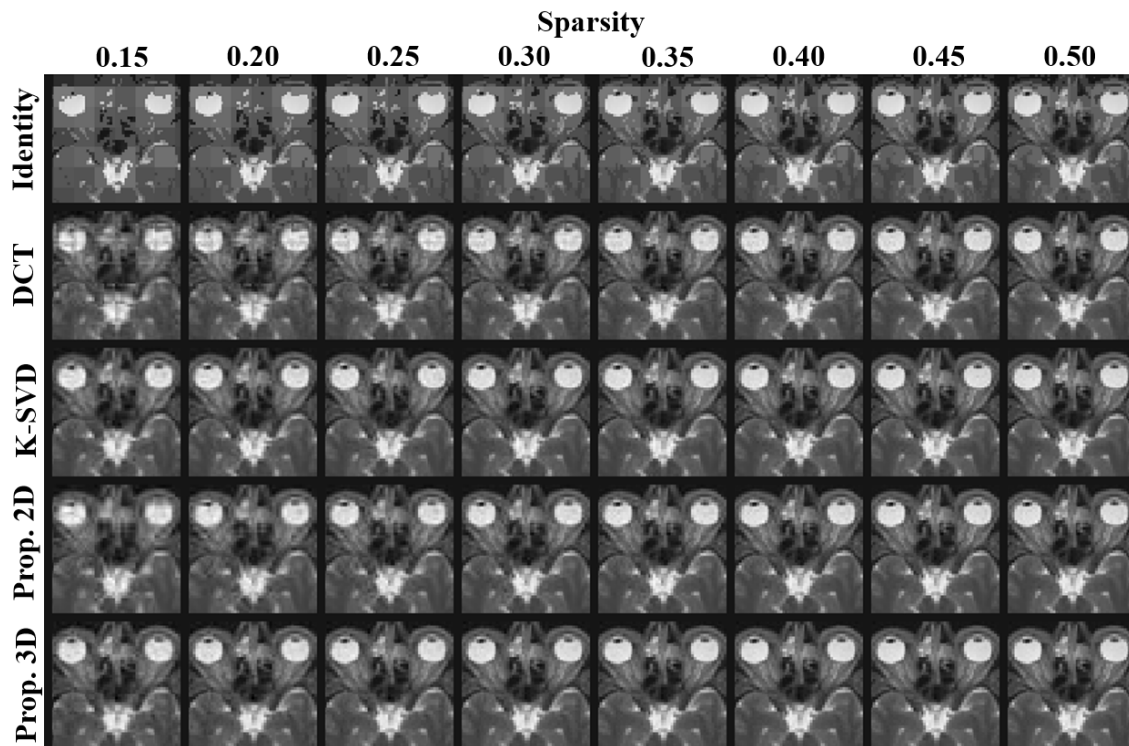


Figure 6 Comparison of the 20<sup>th</sup> slice of the MRI database for different sparsity levels

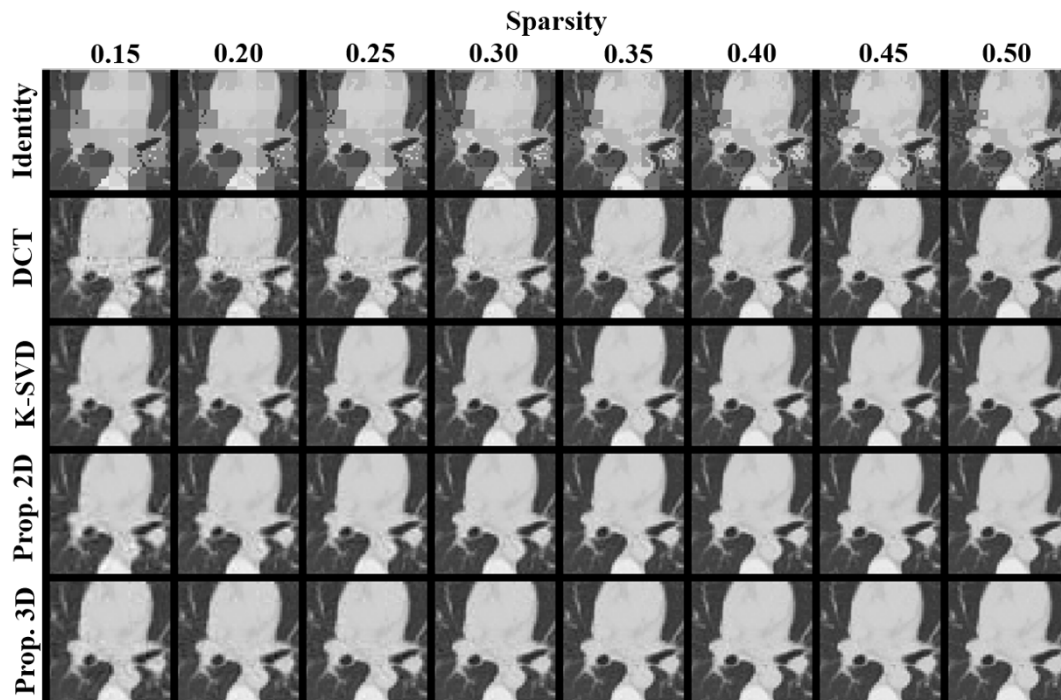


Figure 7 Comparison of the 24<sup>th</sup> slice of the CAT datacube for different sparsity levels

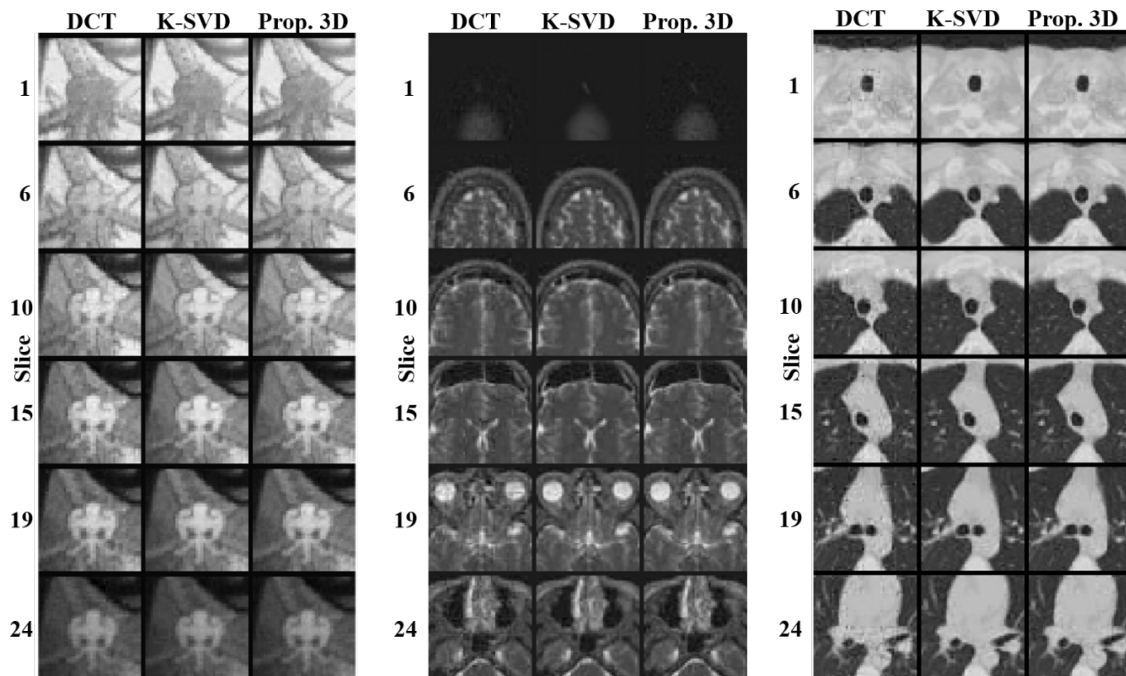


Figure 8 Comparison of the best analytical method (DCT), the K-SVD method and the best proposed method (Prop. 3D), for a fixed sparsity level of 0.15 (15%). Different slices of the multidimensional images are shown to evaluate the quality along the third dimension

### 3.3. Experiment #3: Concentration of the non-zero coefficients (sparsity)

This experiment analyzes the concentration of the non-zero values of the signals after being represented on the

trained dictionaries. For each multidimensional sparse representation in each dictionary, a threshold is applied to remove the values close to zero, in order to observe the non-zero coefficients with higher magnitudes; that is, the most representative coefficients. Table 2 shows a comparison of

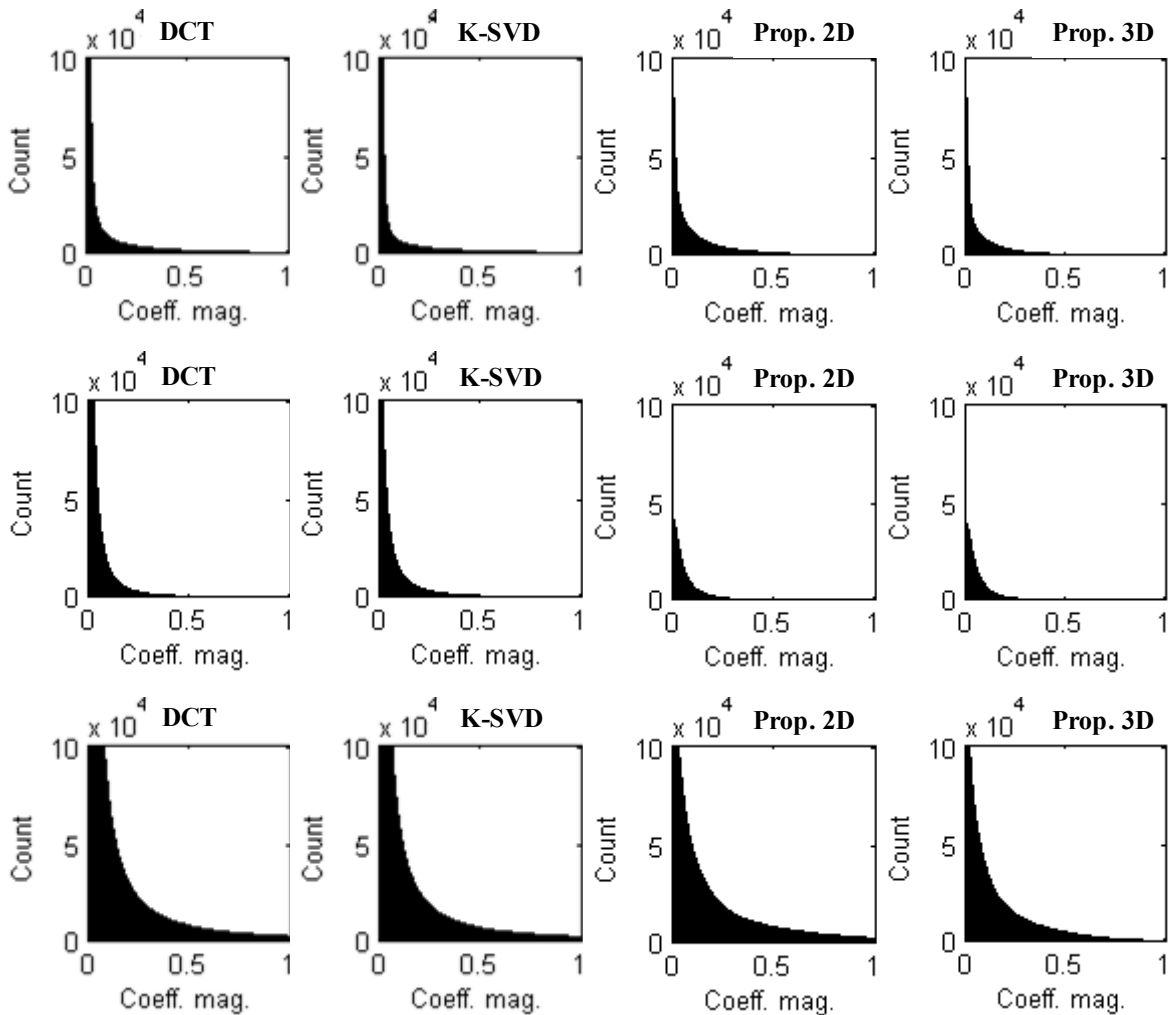
the number of non-zero coefficients attained after applying a threshold to the normalized magnitudes lower than 0.03. It can be observed that the number of non-zero coefficients is lower for the learned dictionaries than that of the DCT, and between the learned dictionaries, the proposed method using 3D patches attain the sparsest representations.

Figure 9 shows the count of the non-zero coefficients for the 4 used dictionaries after being applied to the three multidimensional databases. It can be observed from the figure that the analytical transform generates representations with more non-zero coefficients and with small magnitudes (near to zero) than the representations obtained through the use of the trained dictionary. This means that the representations obtained through the trained

dictionaries are better for sparsifying multidimensional signals than the analytical transforms considered.

**Table 2** Number of non-zero coefficients with normalized magnitude greater than 0.03, obtained by representation of the databases using the 4 dictionaries

	DCT	K-SVD	Prop. 2D	Prop. 3D
HSI	63854	28540	31366	25549
MRI	107129	30957	31182	30523
CAT	315536	114402	105368	92711



**Figure 9** Count of the sparse coefficients generated by the different methods for the three databases. (First row) HSI image. (Second row) MRI image. (Third row) CAT image

## 4. Conclusions

An algorithm for learning sparsifying transforms of multidimensional signals has been proposed in this

manuscript. The proposed algorithm alternates between a sparse coding step solved by hard thresholding, and an updating dictionary step solved by a conjugate gradient method. Two variations of the algorithm using 2D and 3D

patches were shown to process the multidimensional signals adequately, in terms of quality of the reconstruction for different test databases. The proposed algorithm was compared against analytical transforms such as the DCT, and the state of the art K-SVD dictionary learning algorithm. The proposed algorithm using 3D patches showed to have in general a better performance for the representation of the multidimensional images tested in this paper, both in terms of PSNR of the reconstructions and in terms of concentration of the non-zero elements, that is, the proposed method entails better sparse representations.

## 5. Acknowledgements

The authors gratefully acknowledge the Vicerrectoría de Investigación y Extensión of the Universidad Industrial de Santander for supporting this research registered under the project title: Diseño y simulación de una arquitectura de un solo detector en tomografía computarizada, para el muestreo compresivo de imágenes de Rayos-X, (VIE code: 1892). Hoover Rueda is supported by a Colciencias-Fulbright scholarship.

## 6. References

1. J. Bushberg, J. Seibert, E. Leidholdt, and J. Boone, *The essential physics of medical imaging*, 3<sup>rd</sup> ed. Philadelphia, USA: Lippincott Williams & Wilkins, 2011.
2. Ó. Espitia, Y. Mejía, and H. Arguello, "Tomografía computarizada: proceso de adquisición, tecnología y estado actual," *Tecnura*, vol. 20, no. 47, pp. 119–135, 2016.
3. G. A. Shaw and H. K. Burke, "Spectral Imaging for Remote Sensing," *Lincoln Laboratory Journal*, vol. 14, no. 1, pp. 3–28, 2003.
4. A. Camacho, C. Vargas, F. Rojas, S. Castillo, and H. Arguello, "Aplicaciones y retos del sentido remoto hiperespectral en la geología colombiana," *Facultad de Ingeniería*, vol. 24, no. 40, pp. 17–29, 2015.
5. G. R. Arce, D. J. Brady, L. Carin, H. Arguello, and D. S. Kittle, "Compressive Coded Aperture Spectral Imaging: An Introduction," *IEEE Signal Processing Magazine*, vol. 31, no. 1, pp. 105–115, 2014.
6. E. J. Candes and T. Tao, "Decoding by linear programming," *IEEE Transactions on Information Theory*, vol. 51, no. 12, pp. 4203–4215, 2005.
7. E. Candès and M. Wakin, "An Introduction To Compressive Sampling," *IEEE Signal Processing Magazine*, vol. 25, no. 2, pp. 21–30, 2008.
8. S. Qaisar, R. M. Bilal, W. Iqbal, M. Naureen, and S. Lee, "Compressive sensing: From theory to applications, a survey," *Journal of Communications and Networks*, vol. 15, no. 5, pp. 443–456, 2013.
9. A. Bruckstein, D. Donoho, and M. Elad, "From Sparse Solutions of Systems of Equations to Sparse Modeling of Signals and Images," *SIAM Rev.*, vol. 51, no. 1, pp. 34–81, 2009.
10. M. Elad, M. A. T. Figueiredo, and Y. Ma, "On the Role of Sparse and Redundant Representations in Image Processing," *Proceedings of the IEEE*, vol. 98, no. 6, pp. 972–982, 2010.
11. G. Kutyniok, "Theory and applications of compressed sensing," *GAMM-Mitteilungen*, vol. 36, no. 1, pp. 79–101, 2013.
12. S. Mallat, *A Wavelet Tour of Signal Processing*, 1<sup>st</sup> ed. London, UK: Academic Press, 1999.
13. R. Rubinstein, A. M. Bruckstein, and M. Elad, "Dictionaries for Sparse Representation Modeling," *Proceedings of the IEEE*, vol. 98, no. 6, pp. 1045–1057, 2010.
14. M. Elad, P. Milanfar, and R. Rubinstein, "Analysis versus synthesis in signal priors," *Inverse Problems*, vol. 23, no. 3, p. 947–968, 2007.
15. D. L. Donoho, "Compressed sensing," *IEEE Transactions on Information Theory*, vol. 52, no. 4, pp. 1289–1306, 2006.
16. R. Rubinstein, T. Faktor, and M. Elad, "K-SVD dictionary-learning for the analysis sparse model," in *IEEE International Conference on Acoustics, Speech and Signal Processing (ICASSP)*, Kyoto, Japan, 2012, pp. 5405–5408.
17. M. Aharon, M. Elad, and A. Bruckstein, "K-SVD: An Algorithm for Designing Overcomplete Dictionaries for Sparse Representation," *IEEE Transactions on Signal Processing*, vol. 54, no. 11, pp. 4311–4322, 2006.
18. M. Yaghoobi, T. Blumensath, and M. E. Davies, "Dictionary Learning for Sparse Approximations With the Majorization Method," *IEEE Transactions on Signal Processing*, vol. 57, no. 6, pp. 2178–2191, 2009.
19. R. Rubinstein, T. Peleg, and M. Elad, "Analysis K-SVD: A Dictionary-Learning Algorithm for the Analysis Sparse Model," *IEEE Transactions on Signal Processing*, vol. 61, no. 3, pp. 661–677, 2013.
20. M. Yaghoobi, S. Nam, R. Gribonval, and M. E. Davies, "Constrained Overcomplete Analysis Operator Learning for Cosparsity Signal Modelling," *IEEE Transactions on Signal Processing*, vol. 61, no. 9, pp. 2341–2355, 2013.
21. M. Yaghoobi, S. Nam, R. Gribonval, and M. E. Davies, "Noise aware analysis operator learning for approximately cosparsity signals," in *IEEE International Conference on Acoustics, Speech and Signal Processing (ICASSP)*, Kyoto, Japan, 2012, pp. 5409–5412.
22. S. Ravishanker and Y. Bresler, "Learning Sparsifying Transforms," *IEEE Transactions on Signal Processing*, vol. 61, no. 5, pp. 1072–1086, 2013.
23. J. Nocedal and S. Wright, *Numerical Optimization*, 2<sup>nd</sup> ed. New York, USA: Springer, 2006.
24. H. F. Rueda and H. Arguello, "Spatial super-resolution in coded aperture-based optical compressive hyperspectral imaging systems," *Revista Facultad de Ingeniería Universidad de Antioquia*, no. 67, pp. 7–18, 2013.
25. M. J. Ackerman, *The Visible Human Project*, 1994. [Online]. Available: [https://www.nlm.nih.gov/research/visible/getting\\_data.html](https://www.nlm.nih.gov/research/visible/getting_data.html). Accessed on: Apr. 26, 2016.
26. R. G. Lyons, *Understanding Digital Signal Processing*, 3<sup>rd</sup> ed. New Jersey, USA: Prentice Hall, 2011.